IEEE Access
Multidisciplinary ⋮ Rapid Review ⋮ Open Access Journal

Received 5 August 2024, accepted 14 August 2024, date of publication 19 August 2024, date of current version 28 August 2024.

*Digital Object Identifier 10.1109/ACCESS.2024.3446190*

RESEARCH ARTICLE

# Brain Tumor Detection Based on Deep Features Concatenation and Machine Learning Classifiers With Genetic Selection

**MOHAMED WAGEH[1], KHALID AMIN[1], ABEER D. ALGARNI[2], AHMED M. HAMAD[1], AND MINA IBRAHIM[3]**

[1]Department of Information Technology, Faculty of Computers and Information, Menoufia University, Shebeen El-Kom, Menoufia 32511, Egypt
[2]Department of Information Technology, College of Computer and Information Sciences, Princess Nourah Bint Abdulrahman University, P.O. Box 84428, Riyadh 11671, Saudi Arabia
[3]Department of Machine Intelligence, Faculty of Artificial Intelligence, Menoufia University, Shebeen El-Kom, Menoufia 32511, Egypt

Corresponding author: Mohamed Wageh (Mohammed.wageh@ci.menofia.edu.eg)

This work was supported by the Princess Nourah Bint Abdulrahman University Researchers Supporting Project, Princess Nourah Bint Abdulrahman University, Riyadh, Saudi Arabia, under Grant PNURSP2024R51.

**ABSTRACT** The development of brain tumors is often a result of cellular abnormalities, making it a leading factor contributing to mortality among both adults and children on a global scale. However, early detection of tumor can potentially prevent millions of deaths. In this regard, Magnetic Resonance Imaging (MRI) has become a pivotal tool for early brain tumor detection, It holds a vital significance role in enhancing tumor visibility that facilitates subsequent treatment planning and intervention. This research focuses on early stage brain tumor detection, proposing a Computer-Aided Detection (CAD) system that leverages MRI. Utilizing transfer learning, multiple pre-trained deep convolutional neural networks namely VGG-16, Inception V3, ResNet-101, and DenseNet- 201 are used to extract deep features from brain MRI images. Subsequently, the extracted deep features are concatenated and subjected to a genetic algorithm, acting as a technique for feature selection to determine the most important features. These features undergo evaluation using various machine learning classifiers. Two open-access brain MRI datasets, Navoneel brain tumor and Br35H Brain Tumor Detection datasets, are employed to assess model performance. Multiple experiments were conducted using the two datasets: one without feature concatenation or selection, and the other with both processes applied. The experimental results demonstrate that combining and selecting deep features leads to a substantial performance improvement, achieving an accuracy of 99.7% and 99.8% for the first and the second datasets, respectively, that surpasses the other methods.

**INDEX TERMS** Brain tumor, MRI, CNN, deep learning, transfer learning, genetic.

## I. INTRODUCTION

Brain tumors have been widely recognized as a major contributing factor to the significant rise in mortality rates, particularly among children, adults, and the elderly. The human brain consisting of billions of cells, is a remarkably intricate organ and a crucial element of the central nervous system. It serves as the control center for coordinating bodily movements, receiving sensory input, and making informed decisions. Subsequently, it sends out the necessary instructions to enable the body to respond accordingly. Consequently, Any kind of brain abnormality has the potential to be an extremely serious risk to people's health. Among these abnormalities, brain tumors rank among the most gravest and potentially fatal types of cancer [1]. When a brain tumor expands, It may exert strain on the brain's healthy tissue and disrupt its normal functions. This can cause a variety of problems for the person with the tumor, as the brain controls all of the body's actions and processes. Changes in behavior, movement, heart rate, blood pressure, temperature of the body, and balance of fluids are a few examples of these issues [2]. Benign and malignant are the two basic categories

The associate editor coordinating the review of this manuscript and approving it for publication was Carmelo Militello.

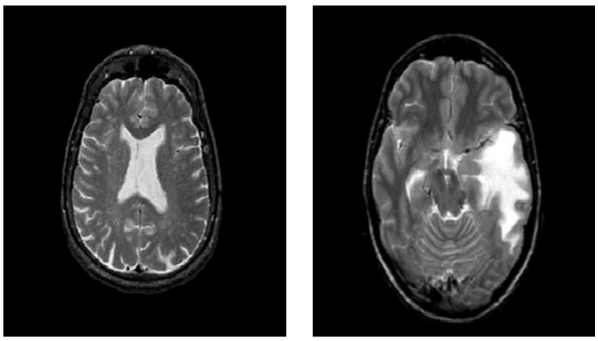

(a) Normal (b) Abnormal

**FIGURE 1.** Normal and abnormal MRI example.

of brain tumors. Benign tumors consist of cancer cells but are considered less damaging because they don't propagate to neighboring cells. On the contrary, Malignant tumors consist of malignant cells that pose a greater risk as they tend to invade nearby tissues and cells. Brain tumors are commonly categorized into different grades ranging from one to four based on their behavior. Grade one tumors, which are less hazardous, are generally associated with longer survival rates. When examined under a microscope, these tumors exhibit an almost normal texture and they tend to grow steadily. Surgery is often considered a viable treatment option for tumors of this grade. When observed under a microscope, grade two tumors display slow growth and show abnormal characteristics. Some of these tumors may recur and spread to nearby tissues, occasionally progressing to higher-grade tumors [3]. While grade three tumors are considered malignant, there is often not a significant distinction between tumors of grades two and three. Grade three tumors typically tend to recur as grade four tumors. Grade four tumors are recognized as the most aggressive form of malignancy. They exhibit rapid growth, display abnormal characteristics under microscopic examination, and effectively infiltrate neighboring brain tissues, triggering the formation of new cancerous cells. Within these tumor cells, areas of dead cells can be observed at the core [4]. Figure 1, illustrates a normal and abnormal MRI images.

Various medical imaging technologies are capable of being used for identifying brain tumors, including computed tomography (CT), positron emission tomography (PET), and magnetic resonance imaging (MRI), which are utilized to visualize and assess internal bodily conditions. Among all of these methods of imaging, MRI is widely considered the most favorable option. It is the only method that is both non-ionizing and non-invasive. that provides useful and high-contrast details about brain tumors [5]. Nevertheless, the manual or visual inspection of these images is a laborious process and takes a considerable amount of time, further complicated by the high influx of patients [6]. This visual review is also prone to human errors, to tackle this problem, there is a need for developing of an automated computer aided detection (CAD) system. Such a system would serve to alleviate the workload associated with the detection of the existence of brain tumors in MRI scans while functioning as a useful tool to assist radiologists and doctors in their tasks.

Considerable efforts have devoted to create and develop a precise and trustworthy solution for the automatic brain tumors detection. However, the presence of substantial variations in shape, texture, and contrast of tumor, continues to pose a difficult challenge in addressing this problem effectively. Conventional machine learning (ML) techniques depend on manually crafted or traditional features, which impose limitations on the the strength and durability of the solution. In contrast, techniques utilizing deep learning autonomously derive significant features, resulting in markedly enhanced performance compared to traditional methods. On the other hand, this techniques necessitate a significant quantity of labeled data for effective training, and obtaining a sufficient quantity of such data poses a significant challenge.

To tackle these challenges, our study introduces a hybrid solution that combines the strengths of different techniques. We utilize pre-trained deep Convolutional Neural Networks (CNNs) as feature extraction models to obtain potent and distinctive deep features from brain MRI scans. These extracted features are then employed with various machine learning classifiers to effectively differentiate between MRI images as normal and abnormal images. Furthermore, this study introduces the suggestion of utilizing concatenated deep features extracted from four distinct pre-trained CNN models. By combining the deep features extracted using multiple CNN models through concatenation, we create a more powerful feature representation. This is because different CNN architectures capture various information and integrating their features enhances the discriminative ability of the representation. To enhance the feature selection process and identify the most impactful features, a genetic algorithm is employed. The concatenated selected deep features are subsequently inputted into the machine learning classifiers to make predictions and determine the final output.

The primary contributions of this research include:

- Designing and introducing an automated hybrid method for brain tumor detection using different pre-trained CNN models to extract deep features from brain MRI images and employing machine learning classifiers to effectively detect brain tumor in MRI images.
- Utilizing a concatenated deep feature vector composed of combinations of the deep features which extracted from the distinct pre-trained CNN models.
- Applying the genetic algorithm as a feature selection technique to identify and utilize the most powerful and important features.

The paper is structured as follows: Section II gives an overview of the previously related work, the presentation of the proposed method is followed in Section III, Section IV presents the experimental results obtained from the conducted research, and lastly, Section V concludes the paper.

## II. RELATED WORK

Early detection of brain tumors holds tremendous significance, leading to the development of various methods by researchers. Several research papers have been published in this field, and some of them will be discussed here. Various methods have been suggested for the automatic classification of brain MRI images, utilizing both traditional machine and deep learning approaches. In the traditional machine learning methods, Feature extraction process is a fundamental step because the classification accuracy is heavily reliant on the quality and relevance of the extracted features.

Shree and Kumar [7] conducted a study where they divided the MRIs of the brain into two classes: one representing normal and the other denoting abnormal. They employed the Gray Level Co-occurrence Matrix (GLCM) for the extraction of features and utilized a probabilistic neural network (PNN) to accurately categorize the MRI images of the brain as either normal or abnormal MRIs, reaching a 95% accuracy rate. Ullah et al. [8] applied the discrete wavelet transformation (DWT) to extract the approximation and detail coefficients through three-level decomposition. They proceeded to decrease the coefficients using color moments (CM) and utilized an artificial feed-forward neural network to Precisely distinguishing between regular and irregular brain MRIs, they achieved an accuracy of 95.8%. Rajan and Sundar [9] introduced an energy-efficient hybrid approach for the automated segmentation and identification and of tumors. Their suggested approach consisted of seven separate stages, reaching a 98% accuracy rate. However, a significant flaw in their approach is the lengthy computational duration, which can be attributed to the utilization of multiple techniques.

A model proposed by Arunachalam and Savarimuthu [10] aimed to differentiate between brain MRI images to categorize them into normal and abnormal categories. Their model consisted of several steps, initially, they enhanced the brain MRI image. Then, they utilized Gabor filters, GLCM, and DWT for feature extraction. Finally, the features that were extracted were inputted into a feed-forward backpropagation neural network, resulting in a high level of accuracy in classifying brain tumors. Gupta et al. [11] combined the texture features extracted from three different techniques, the GLCM, Local Binary Patterns (LBP), and Gray-Level Run Length (GIRL) methods. They applied diverse machine learning classification algorithms to differentiate and categorize MRI images into normal or abnormal categories. The model they suggested demonstrated an average classification accuracy of 97.37%. Minz and Mahobiya [12] proposed a model that integrates image-processing techniques and machine learning algorithms for the purpose of detecting tumors. They utilized the GLCM method for the extraction of the relevant image features. Their classification task was carried out employing the AdaBoost algorithm. The results of their approach demonstrated an accuracy of 89.90% in classifying brain tumors. Minz and Mahobiya [13] used GLCM and by utilizing feed-forward neural networks, the authors successfully characterized tissue and achieved a remarkable tumor diagnosis accuracy of 97.50%.

Arasi and Suganthi [14] introduced a method for effectively distinguishing MRI scans depicting benign and malignant brain tumors. Their suggested approach achieved an impressive accuracy level of 97.69%. The method consisted of several stages, including Segmentation of tumors employing a fuzzy clustering algorithm, extracting features utilizing GLCM, and implementing classification through the Boosting Support Vector Machine. Soltaninejad et al. [15] employed a diverse set of textural features and utilized the superpixel approach to differentiate between images with tumors and those without tumors. Their method yielded an accuracy rate of 98.28%. Nabizadeh and Kubat [16] Employed the Complex Wavelet Transform (CWT) in conjunction with statistical features and the Skippy greedy snake technique to categorize brain tumors. They assessed the effectiveness of their approach using a dataset consisting of simulated images and 96.80% accuracy was reported in tumor detection. Wageh et al. [17] Utilized machine learning approaches to boost the accuracy of classification. GLCM and LBP are employed for feature extraction, and feature selection is carried out through the utilization of Principal Component Analysis (PCA) and Information Gain (IG) algorithms. Various machine learning classifiers are utilized to classify MRI images that depict the presence of tumors and those that do not. The results demonstrate a high accuracy of 98% when combining the GLCM and LBP features.

Over the past decade, Deep learning techniques have become notably prominent in the realm of classifying brain MRIs. Unlike traditional approaches, deep learning methods eliminate the need for manually crafted features by incorporating both the feature extraction step and the classification process into the self-learning procedure. To apply the deep learning approach, it is necessary to have a large dataset, and in certain instances, preprocessing tasks may be necessary. Following that, the essential features are autonomously identified within the deep learning model [18].

Deepak and Ameer [19] employed a pre-trained GoogLeNet model to obtain features from the brain MRI scans. They employed a deep Convolutional Neural Network to categorize distinct types of brain tumors. Remarkably, The method they employed resulted in a 98% accuracy rate. Cinar and Yildirim [20] utilized various CNN models, including including ResNet-50, GoogLeNet, Inception V3, DenseNet-201, and AlexNet, for the classification of brain MRI images. They obtained promising accuracy outcomes by employing these models. Specifically, They altered the pre-trained ResNet-50 CNN architecture by eliminating the final five layers and incorporating new eight layers into the modified model, They attained an accuracy rate of 97.2% in their classification task. Khawaldeh et al. [21] introduced a CNN model for dividing brain MRIs into two categories normal and abnormal, Additionally, differentiating between high and low glioma tumor grades

is also addressed. They introduced alterations to the initial AlexNet model and utilized it as the framework for their network, their method produced a 91% accuracy rate. Saxena et al. [22] employed transfer learning techniques to categorize brain tumor data using the VGG-16, ResNet-50, and Inception V3 models. With an a 95% accuracy rate, the ResNet-50 model outperformed the other models. Swati et al. [23] utilized three distinct CNN architectures for the brain tumor classification. The VGG19, VGG16, and AlexNet architectures demonstrated accuracy rates of 94.82%, 94.65%, and 89.95%, respectively.

Diaz-pernas et al. [24] introduced a CNN architecture with multiple pathways designed to automatically segment brain tumors, Meningioma, glioma, and pituitary tumors are included. Their suggested approach was Underwent assessment using a publicly accessible dataset of T1-weighted contrast-enhanced MRI scans, achieving a 97.3% accuracy rate. Noreen et al. [25] utilized various CNN architectures to extract features. which were then categorized using machine learning algorithms, Inception V3 model yielded the highest accuracy rate of 94.3%. Kang et al. [26] presented a technique for classifying MRI images of the brain that makes use of deep features ensemble. The process involves three primary phases. Initially, the input images go through pre-processing. The processed images are then inputted into various pre-trained CNN models for feature extraction. The extracted features are later utilized as input for diverse machine learning classifiers, Furthermore, their research identifies three pre-trained models that demonstrate the most favorable outcomes. These best-performing pre-trained models' extracted features are merged into a single sequence. Ultimately, the machine learning classifiers are trained using the combined features. According to the findings, ResNeXt-50, Inception-v3, and DenseNet-169 generated the best features for the classification process.

Özbay and Özbay [27] suggested a hybrid CNN approach, incorporating the mRMR (minimum-redundancy maximum-relevance) method, machine learning methods were utilized to classify brain MRI scans. Different deep learning architectures were used as feature extractors. The best-performing designs for feature extraction were found to be DenseNet201, EfficientNet-B0, and DarkNet53. The features extracted are combined and refined through the mRMR technique, with the utilization of SVM, KNN, and Ensemble algorithms as classification methods. The classification results demonstrate an accuracy rate of 99.6% when using the SVM. Mahmoud et al. [28] utilized CNN models to detect brain tumor in MRI images. The optimization of the models was achieved through the utilization of Aquila Optimizer (AGO), streamlining the creation and adjustment of the initial population tailored to the chosen dataset, In particular, the brain tumor dataset was trained and validated using the VGG-16, VGG-19, and Inception-V3 convolutional neural network (CNN) architectures, in combination with the AQO optimizer. Notably, The VGG-19 model attained the highest level of accuracy, boasting an impressive accuracy rate of 98.95%.

Anantharajan et al. [29] introduced a novel method for detecting brain tumors in MRI images using deep learning and machine learning. The MRI images are preprocessed with an Adaptive Contrast Enhancement Algorithm and a median filter, then segmented using fuzzy c-means. Features like energy, mean, entropy, and contrast are extracted via the Gray-Level Co-Occurrence Matrix. An Ensemble Deep Neural Support Vector Machine classifier is used to identify abnormal tissues, achieving an accuracy of 97.93%. Rahman and Islam [30] introduced a novel parallel deep convolutional neural network (PDCNN) topology to extract global and local features while addressing over-fitting with dropout regularization and batch normalization. Images are resized and converted to grayscale, followed by data augmentation to increase the dataset size. The model combines two simultaneous deep convolutional neural networks with different window sizes to capture both local and global information. Tested on three types of MRI datasets, the method achieved accuracies of 97.33%, 97.60%, and 98.12%. Khaliki and Başarslan [31] objective was to classify brain tumors, specifically glioma, meningioma, and pituitary tumors, from brain MR images. They utilized CNN and CNN-based models like Inception-V3, EfficientNetB4, VGG19, along with transfer learning methods for classification. The VGG16 model achieved the highest accuracy at 98%.

In summary, it demonstrated that significantly higher accuracies are obtained when utilizing deep learning techniques compared to traditional machine learning methods. However, It is significant to keep in mind that in order for deep learning models to perform better than conventional machine learning methods, they usually need an extensive amount of training data. For further clarification, Table 1 provides a comprehensive comparison delineating the Pros and Cons of the previous related work. To overcome this limitation, the proposed work aims to introduce an approach that integrates both deep learning models and machine learning algorithms. The approach utilizes a concatenated deep feature vector composed of combinations of the deep features extracted from the distinct CNN models to have the advantage of the integration of diverse visual information captured by the different models, it also employs a genetic algorithm to optimize features and select the most powerful and important features due to its capacity to cope with and handle a wide range of features, thereby optimizing the performance of the hybrid model.

## III. PROPOSED METHOD

The suggested method's primary goal is the detection of brain tumors in MRI scans. This work introduces a brain tumor detection method that utilizes normal and abnormal MRI brain images. An extensive explanation of the general architecture of our proposed method is given in this section. The visual representation of the proposed method for

**TABLE 1. Comparison of the Related work Pros and Cons.**

| Ref | Pros | Cons |
|---|---|---|
| [7] | Achieved high accuracy (nearly 100% for trained datasets, 95% for tested datasets). | Limited exploration of other effective classifiers beyond PNN. |
| [8] | Attained 95.8% accuracy with a simple method; Enhanced image quality via median filtering and CLAHE for better feature extraction. | Generalizability across diverse datasets and clinical scenarios not well-established. |
| [9] | Integrated K-means clustering with Fuzzy C-Means and active contour for effective segmentation; Improved accuracy through intensity adjustment. | Limited coverage of scenarios due to limited dataset size and variety. |
| [10] | Extracts and utilizes various texture features (GLCM, Gabor, and DWT) for classification; Achieved high classification accuracy of 97.05% on average. | Limited dataset size for comprehensive evaluation. |
| [11] | Implemented a three-level classification system,starting with tumor detection, then location, and finally type; Utilized multiple texture features (LBP, GLCM, GIRL); Improved performance in tumor detection and location. | Unclear explanation of segmentation techniques; Limited generalizability to diverse datasets. |
| [13] | Achieved high classification accuracy of 97.5% for 4 different brain tumor; Used well-established GLCM textural features for feature extraction | Limited dataset size for broader validation. |
| [14] | Used genetic optimized median filter and hierarchical fuzzy clustering for achieving 97.69% accuracy on BraTS dataset. | Evaluation focused on a specific dataset; Unclear generalizability to other medical images. |
| [15] | Employed superpixel technique with novel features (textons, fractals, curvatures) achieving robust performance on BRATS 2012 dataset. | Validation primarily on single dataset; Parameter optimization parameters (e.g. superpixel size, compactness factor) needed for different datasets. |
| [16] | Combined texture and contour-based techniques for tumor segmentation with high accuracy; Utilized an extensive set of initial features, including statistical and wavelet-based, to capture diverse texture information | Limited validation on diverse datasets and clinical scenarios; The criteria used for selecting the top features with the highest weights from the Winnow algorithm are not clearly explained |
| [17] | Utilized combined feature vector of LBP and GLCM features with the use of feature selection, achieving 98% accuracy. | Evaluation on a limited dataset; Needs validation on larger and diverse datasets; Lack of comparison with state-of-the-art methods. |
| [19] | Applied deep transfer learning for 3-class brain tumor classification, showing significant performance improvement over state-of-the-art methods. | Performance limitation with softmax classifier; Dataset size may affect robustness; Weaknesses observed in meningioma class due to fewer samples. |
| [20] | Utilized transfer learning by fine-tuning a pre-trained ResNet50 model, which can be a more efficient approach than training from scratch and achieved 97.01% accuracy in brain tumor classification from MRI images. | Need for larger datasets to confirm model performance. |
| [21] | Achieves high accuracy of 91.16% in classifying healthy, low-grade, and high-grade tumors; Novel application of transfer learning by modifying the popular AlexNet CNN architecture | Insufficient details on CNN model architecture and parameters; - Limited dataset size (only 130 subjects). |
| [22] | Attained 95% accuracy with ResNet-50 model for brain tumor classification; Utilized transfer learning with pre-trained CNN models, minimizing training time and data requirements. | Limited evaluation on a larger and more diverse dataset. |
| [23] | Achieved 94.82% accuracy using block-wise fine-tuning of pre-trained CNNs, which can be more efficient and effective than layer-wise fine-tuning. | Unclear explanation of block-wise fine-tuning; Generalizability to different datasets and clinical scenarios not well-established. |
| [24] | A multiscale method inspired by the human visual system extracts distinctive features at various scales; Fully automatic technique requires no preprocessing, such as skull stripping, and achieves a high tumor classification accuracy of 97.3%. | Presence of non-cerebral areas like skull and vertebral column can lead to false positives. |
| [25] | Used fine-tuned Inception-V3 and Xception models for feature extraction achieving 94.34% accuracy with the Inception-V3 ensemble model. | Dataset size may introduce bias; Limited generalizability. |
| [26] | Achieved high accuracy using ensemble of deep features with transfer learning; Utilizes pre-trained CNN models through transfer learning, reducing the need for extensive training time and large datasets | Bias potential towards specific tumor types due to dataset limitations that might not represent the full diversity of brain tumors in terms of subtypes, grades, and imaging characteristics. |
| [27] | Combined multiple CNN architectures for feature extraction, capturing different aspects of tumor characteristics. | Unclear performance across diverse datasets and clinical scenarios. |
| [28] | Employed transfer learning with pre-trained CNN models, reducing both training time and data needs. | Limited evidence of performance on varied datasets and clinical scenarios. |
| [29] | Proposed EDN-SVM model Integrates the strengths of DNN and SVM and achieved 97.93% accuracy. | Needs a substantial amount of training data to perform optimally. |
| [30] | Extracted local and global features using two parallel convolutional networks with different window sizes. | Utilized a relatively small training dataset, potentially insufficient for building a robust model that generalizes well to new, unseen data. |
| [31] | presented a valuable comparison of different CNN architectures and achieved up to 98% accuracy with VGG16. | Dataset size may affect model robustness against unseen data. |

detecting brain tumors is represented in Figure 2, illustrating the architecture utilized in our method. First, the input MRI images undergo pre-processing, which involves several operations such as cropping, resizing, augmentation, and filtering. These steps are performed before feeding the images into the models. Next, the Pre-processed images are utilized as the input for the pre-trained CNN models, where these models operate as tools for extracting features. These models

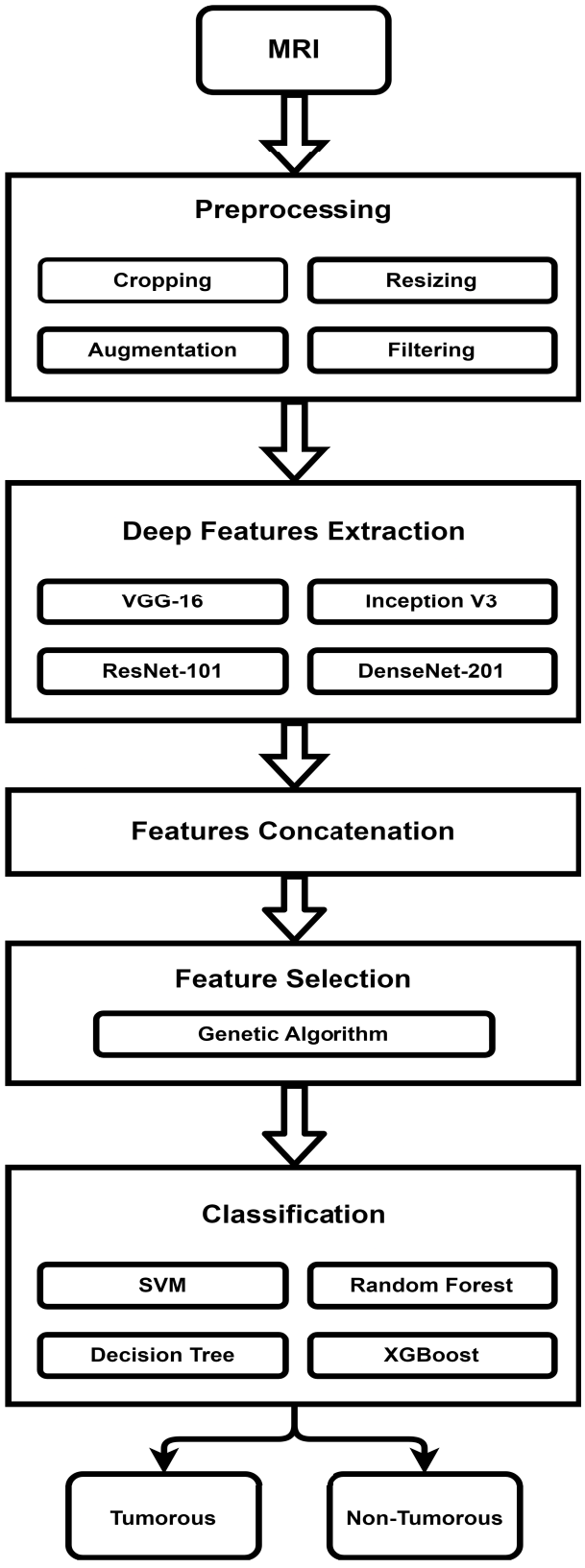


**FIGURE 2.** Proposed Method Block Diagram.

are employed for the purpose of extracting features. In the subsequent step, the obtained features from the different pre-trained CNN models are combined or concatenated together. Following that, a genetic algorithm is employed on the combined features as a method for selecting features. The selected features are then utilized as input for the machine learning classifiers to carry out the classification process.

### A. DATASET

Brain MRI images contain essential information for distinguishing different brain tissues, making brain tumor detection a prominent research field for both medical and image-processing professionals. MRI scans offer several advantages such as being non-invasive, radiation-free, multi-directional, and providing multi-dimensional identification. These advantages make MRI superior to other alternative medical imaging methods such as CT scans and X-rays in the medical field, ensuring patient safety and accurate diagnostic capabilities [32].

The proposed method was applied to two distinct brain MRI datasets with the aim of detecting brain tumors. The first dataset is the Navoneel brain tumor dataset, referred to as Dataset I for simplicity, which was obtained from the Kaggle website [33]. It consists of 253 brain MRI images, out of which 155 exhibit tumors and the remaining 98 are tumor-free. The second one is Br35H Brain Tumor Detection, also referred to as Dataset II for simplicity [34], was also acquired from Kaggle. It includes 3000 images, half of which exhibit tumors, while the remaining 1500 images are tumor-free.

### B. PREPROCESSING

Image preprocessing is essential for preparing images before they are fed into algorithms or models for any task. It helps to remove noise, standardize image characteristics, and enhance important features. By applying preprocessing techniques, the images become more suitable for the desired tasks. It allows for better accuracy, improved performance, and more reliable results, Therefore, image preprocessing serves as a critical step in optimizing the interpretation and usability of images for various purposes. In this research, the improvement of brain MRI image quality was pursued through a data preprocessing procedure comprising four fundamental steps, represented as follows:

- **Cropping**
  In the used datasets of brain MRI images, a majority of these images exhibit undesirable areas and spaces, which adversely impact the classification performance. Therefore, it becomes imperative to crop the images, eliminating unwanted regions and retaining only the relevant information for improved classification accuracy, Hence, the utilization of cropping on the MRI datasets was an essential step.
- **Resizing**
  Considering the varying dimensions and sizes of the MRI images within the used dataset, it is recommended to adjust their dimensions to a consistent width and

height for optimal outcomes. In this study, we performed resizing of the MRI images to either 224 × 224 or 299 × 299 pixels. This choice is consistent with the specified image dimensions needed for pre-trained CNN models, which typically expect images of size 224 × 224 pixels, with the exception of Inception V3, which necessitates input images of size 299 × 299 pixels. By resizing the images to these standardized dimensions, we ensure compatibility with the pre-trained models and facilitate consistent and reliable processing [26].

- **Augmentation**
  Considering the relatively small size of the used MRI dataset, Image augmentation techniques are employed. Image augmentation involves generating an augmented dataset by applying various modifications to the original images. This process involves generating numerous duplicates of the initial image with alterations in orientations, scales, locations, brightness, and other attributes. Research suggests that the augmentation of the existing data, instead of gathering new additional data, can enhance the classification accuracy of the model [26]. By leveraging image augmentation, we aimed to expand the variability and diversity of our dataset, thereby enhancing the generality and resilience of the model.
  In our image augmentation process, several augmentation techniques are utilized including Horizontal flipping, Vertical flipping, Rotation, Horizontal shifting, and Vertical shifting. These techniques involve manipulating the images in various ways. Flipping an image horizontally involves reflecting it around a horizontal axis, whereas vertical flipping entails reflecting it around a vertical axis. Rotation rotates the image by an angle within the range of -20 to 20 degrees. Additionally, Horizontal and Vertical shifting moves the image horizontally and vertically within the range of -20 to 20 pixels. By applying these augmentation strategies, we aimed to introduce additional variations and diversify the dataset.
- **Filtering**
  To preserve the quality of input brain MRI dataset images while reducing noise, we employed the median filter. The median filter is a nonlinear filter that operates by finding the median value among the pixels within the filter mask. Every pixel is individually processed and substituted with the median brightness value of its local neighborhood. This approach effectively minimizes noise without causing blurring of edges or loss of picture details. The strength of the median filter lies in its resistance to outliers, as the median value is robust and not influenced by extreme values. This property ensures that the filtered pixels retain their realistic appearance. Moreover, the median filter preserves fine high-frequency details, making it a valuable tool for noise reduction in brain MRI images [35].

### C. EXTRACTION OF DEEP FEATURES USING PRE-TRAINED CNN MODELS

CNNs, classified as deep neural networks, leverage convolutional layers to filter input data to extract relevant information. The CNN's convolutional layers utilize convolutional filters that process the input, generating the output of neurons linked to localized regions within the input. This mechanism enables CNNs to extract temporal and spatial features from images. Moreover, the convolutional layers utilize a method of weight-sharing, effectively decreasing the total number of parameters involved [36], [37].

CNNs consist of three primary components, first, a convolutional layer that focuses on extracting temporal and spatial characteristics, second, a subsampling layer (also known as max-pooling) that aims to reduce the size of the input image's dimensions, and third, a fully connected (FC) layer is tasked with categorizing the input image into distinct classes. Figure 3 illustrates the the CNN architecture.

#### 1) TRANSFER LEARNING

Typically, CNNs demonstrate superior performance when applied to larger datasets compared to smaller ones. However, in scenarios where generating a sizable dataset for training is impractical, transfer learning can be employed. Transfer learning entails using a pre-trained model, which has been trained on extensive benchmark datasets like ImageNet, as a a tool for extracting features in other tasks involving a comparatively smaller dataset, like an MRI dataset [38]. By Utilizing transfer learning substantially diminishes the time and effort required for training deep learning models from scratch. Additionally, the necessity for a large dataset for training the model is mitigated [39]. Figure 4 shows the idea of the Transfer Learning.

#### 2) EXTRACTION OF DEEP FEATURES

In this research, CNN-based models are used to serve as feature extractors, this approach allowed us to capture significant features from the data without requiring human supervision. Additionally, due to the relatively not large MRI dataset and the the challenges associated with training and optimizing deep CNN models from scratch, a transfer learning-based approach is adopted. This involved utilizing pre-trained CNN models on an extensive ImageNet dataset for the extraction of deep features from our brain MRI images. This approach facilitates efficient and effective feature extraction, even with a smaller dataset, enhancing the overall performance and capabilities of our model.

For our study, pre-trained CNN models are employed, namely VGG-16, Inception V3, ResNet-101, and DenseNet-201. These models are utilized as deep feature extractors. The extracted deep features using these models are then concatenated and inputted into machine learning classifiers.

- **VGG-16**
  Also referred to as the Visual Geometry Group 16, it is a CNN architecture that has shown remarkable

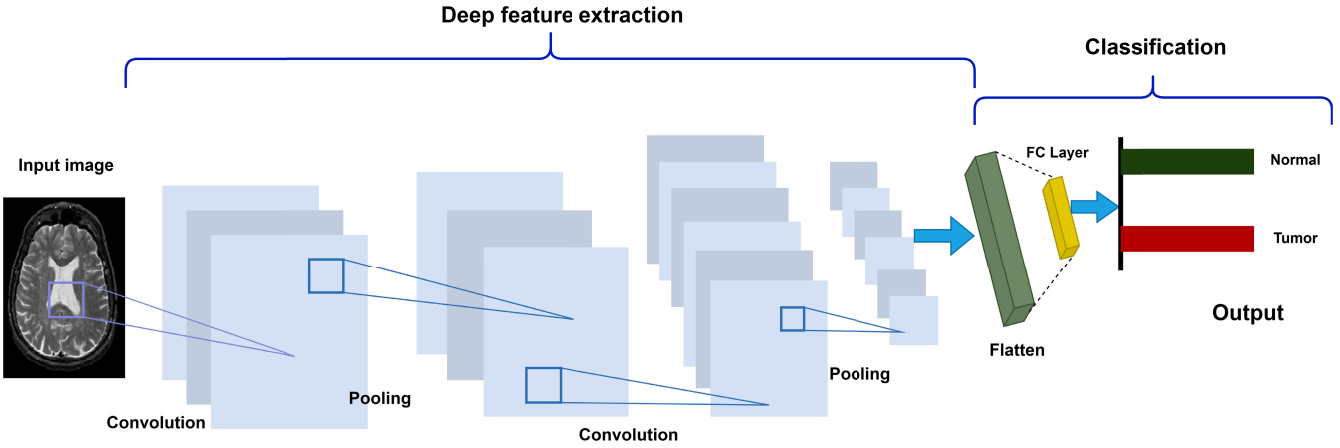


**FIGURE 3.** CNN Architecture.

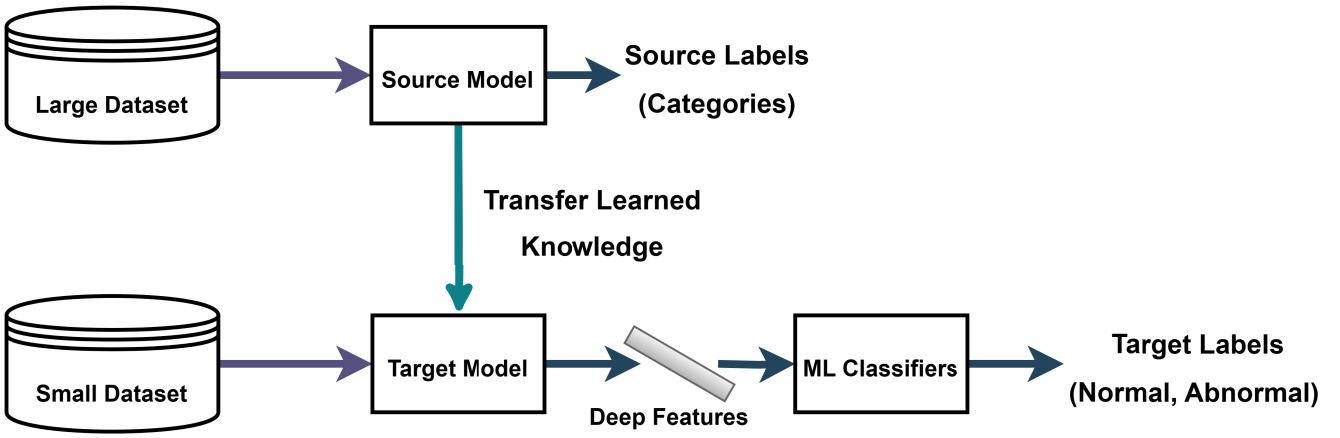


**FIGURE 4.** Transfer Learning Idea.

results in various tasks of computer vision. It was introduced by Simonyan and Zisserman [40]. The VGG-16 architecture is characterized by its deep structure, consisting of a total of sixteen layers, comprising both convolutional and fully connected layers. It features small 3 × 3 convolutional filters across the entire network, enabling a deeper network while maintaining a manageable number of parameters. VGG-16 is widely known for its depth and effectiveness in image recognition tasks. The influence it has on the realm of computer vision, particularly in transfer learning, has made it a valuable tool for researchers and practitioners. VGG-16 exhibits strong capabilities in image recognition tasks, particularly Within the realm of diagnostic medical imaging, including MRI images and X-ray. Its ability to categorize and classify images has shown excellent performance in various applications, making it a valuable asset in image detection tasks [28].

- **Inception V3**
  It is a deep CNN architecture designed for tasks related to the classification of images. It was introduced by Szegedy et al. [41]. Inception-v3 has gained significant popularity in the realm of image recognition. This architecture has successfully reduced computational complexity while maintaining a high level of feature expressiveness, enabling efficient extraction of visual features across multiple scales. The effectiveness of Inception-v3 in image recognition has been demonstrated through various analyses. Compared to Inception-v1 and Inception-v2, The enhanced architecture of Inception-v3, coupled with its design of a deeper network and a larger input size of 299, facilitates quicker computations and improved performance [28].
- **ResNet-101**
  It is a deep CNN architecture that has showed remarkable performance in tasks related to recognizing images. It was introduced by He et al. [42]. ResNet-101 is composed of a sequence of convolutional layers with residual blocks. The residual blocks comprise several convolutional layers along with shortcut connections that skip one or more layers. The skip connections enable the gradient flow to bypass directly to the deeper

layers, facilitating the training of deep networks without suffering from degradation issues [42]. The success of ResNet-101 has extended beyond image recognition tasks. Its deep architecture and skip connections make it suitable for transfer learning, where pre-trained ResNet-101 models that have been trained on extensive datasets can be employed as feature extractors for various computer vision tasks.

**TABLE 2. Parameters for the pre-trained CNN models.**

| Parameter | Description |
|---|---|
| weights = 'imagenet' | Loads pre-trained weights from the ImageNet dataset. |
| include_top = False | Excludes the fully connected top layers of the model. |
| pooling = 'max' | Applies max pooling to the output of the last convolutional layer, reducing its spatial dimensions. |

- **DenseNet-201**
  It is a deep CNN architecture that has acquired considerable interest within the realm of computer vision. It was introduced by Huang et al. [43]. The architecture of DenseNet-201 consists of multiple densely connected blocks, each containing multiple convolutional layers. Within each block, each layer's output is combined with the feature maps from all the layers that came before it, which leads to dense feature maps being fed as input to subsequent layers. This dense connectivity pattern enables the network to extract highly discriminative features and encourages feature reuse, leading to improved model performance [43]. It has demonstrated effective results across various tasks of computer vision, Positioning itself as a cutting-edge solution within this domain.

In this study, several key parameters are specified to customize the pre-trained CNN models for our specific task. Table 2 provides a detailed description of these parameters, including the use of pre-trained weights, the inclusion or exclusion of the top layers, and the type of pooling applied.

Following the employing of these four pre-trained models to extract features, the obtained features are then concatenated and proceed through the subsequent phases.

### D. FEATURES CONCATENATION

Concatenation involves combining the extracted features from each model into a one-feature vector, which acts as the input data for subsequent stages in the process. Concatenating the extracted features from different pre-trained models can bring several advantages to the overall system. It allows for the integration of diverse visual information captured by each model. Each model may have specialized in capturing different types of features or patterns, and by concatenating their outputs, a more comprehensive representation can be obtained. Once the features are extracted using the pre-trained models, the concatenation process takes place as an important step in the pipeline.

In our research, deep feature concatenation is carried out at various levels. Firstly, the extracted features from the first two models (VGG-16 and Inception V3) are concatenated. Subsequently, the extracted features from the first three models (VGG-16, Inception V3, and ResNet-101) are concatenated. Lastly, the concatenation included all the deep features extracted from the four models (VGG-16, Inception V3, ResNet-101, and DenseNet-201). Subsequently, the concatenated features are utilized as input for the next step, where the genetic algorithm is employed for feature selection.

### E. FEATURE SELECTION USING GENETIC ALGORITHM

The process of feature selection is a critical step with its primary goal being the identification and selection of a subset of important features from the original set of features. This process helps to improve model performance, reduce computational complexity, enhance interpretability, diminish the count of interrelated, irrelevant, or distracting variables.

In this research, a genetic algorithm is employed for the selection of the most relevant features depending on its evolutionary process, capable of handling a substantial number of features and producing features that embody the most effective solution for a specific dataset. As a result, this approach is anticipated to deliver superior outcomes. As a population based search algorithm, the genetic algorithm simulates the natural evolutionary process. It consists of a set of chromosomes, where each chromosome serving as a possible resolution to the problem being addressed. The population of the genetic algorithm begins with a random initialization. Through iterations, the population is updated using operators like elitism, crossover, and mutation. These operators assist in recognizing, prioritizing, and reorganizing beneficial building blocks found in the parent chromosomes. The ultimate goal is to obtain improved chromosomes with enhanced characteristics [44]. The Fitness score evaluation for each individual in the population is calculated as shown in Equation 1.

$$\text{Fitness score}_i = \frac{1}{n}\sum_{j=1}^{n}\left(\sum_{k=1}^{m}\log(x_{kj}+10^{-8})\cdot x_{kj}\right) \quad (1)$$

where:

- $n$ is the number of samples in the dataset $X$.
- $m$ is the number of selected features (non-zero elements in the feature mask).
- $x_{kj}$ is the value of the $j$-th selected feature for the $k$-th sample in $X$.
- $\log(x_{kj}+10^{-8})$ is the natural logarithm of $x_{kj}$ with a small constant $10^{-8}$ added to prevent taking the log of zero.

The process of genetic feature selection is utilized for the purpose of selecting features from the concatenated deep features. The goal is to identify the most informative subset of features among the concatenated deep features. This approach aims to enhance the overall performance and effectiveness of the selected features. Subsequently, the selected features are utilized as input in the subsequent step

**TABLE 3.** Number of features before and after selection.

| Model | Num. of extracted features | Num. of Dataset I selected features | Num. of Dataset II selected features |
|---|---|---|---|
| VGG-16 | 512 | 208 | 211 |
| Inception v-3 | 2048 | 928 | 925 |
| ResNet-101 | 2048 | 928 | 880 |
| DenseNet-201 | 1920 | 858 | 873 |
| VGG-16 + Inception v-3 | 2560 | 1182 | 1131 |
| VGG-16 + Inception v-3 + ResNet-101 | 4608 | 2157 | 2107 |
| VGG-16 + Inception V-3 + ResNet-101 + DenseNet-201 | 6528 | 3174 | 3043 |

for machine learning classifiers. Table 3 presents information regarding the dimensions of extracted and concatenated features both before and after undergoing the selection process that effectively demonstrates substantial feature reduction.

### F. CLASSIFICATION

In the classification (detection) process, the selected subset of the concatenated deep features serves as input for various machine learning classifiers. This study employs four different classifiers, namely Support Vector Machine (SVM), Random Forest (RF), Decision Tree (DT), and Extreme Gradient Boosting (XGB), to perform the classification task.

- **Support Vector Machine (SVM)**
  SVM is a commonly employed machine learning classifier renowned for its excellent performance in various classification tasks, The SVM's goal is to identify an ideal hyperplane that effectively maximizes the distance between data points belonging to distinct classes. SVM represents a predictive analysis algorithm characterized by the utilization of kernels, which constitute a class of algorithms designed for the analysis of patterns. The significance of kernels in SVM lies in their pivotal role in transforming input data into a suitable format, thereby enhancing the effectiveness of analysis [45].
- **Random Forest (RF)**
  RF is an ensemble classifier integrates multiple decision trees to formulate predictions. It employs the method of majority voting to obtain the final result. By utilizing different subsets of the same training dataset across multiple trees, Random Forest reduces overfitting, minimizes variance, and enhances performance. This averaging of multiple decision trees helps to balance bias and improve overall predictive accuracy [46].
- **Decision Tree (DT)**
  DT operates similarly to conditional control statements, conducting decision analysis and research operations. However, in the Decision tree classifier, as trees grow deeper, overfitting becomes a concern. The structure of a Decision Tree resembles a tree, where nodes represent attributes or features that lead to specific outcomes. Each leaf node contains information about the corresponding class label [46].

**TABLE 4.** Hyperparameters Used by The Various Classifiers.

| Classifier | Used Parameters |
|---|---|
| SVM | kernel='rbf', C=0.01, gamma='scale', class_weight='balanced' |
| Random Forest | n_estimators=100, max_depth=100, random_state=42 |
| Decision Tree | criterion='entropy', splitter='random', max_depth=100, min_samples_split=2, min_samples_leaf=1, random_state=42 |
| XGBoost | max_depth=100, learning_rate=0.1, n_estimators=100, subsample=0.001, reg_alpha=0.1 |

- **Extreme Gradient Boosting (XGB)**
  XGB is an ensemble model that integrates both classification and regression tree sets. By combining the power of classification and regression trees, this unique combination allows XGB to function as an ensemble model for classification and regression tasks, leveraging the strengths of both classification and regression trees. It is utilized in the context of supervised learning allowing for improved performance [47].

The selected concatenated MRI brain images were employed to train these classifiers to carry out the classification task, with the main objective being to achieve optimal efficiency. Table 4 provides a summary of the optimal hyperparameter configurations that are utilized by the multiple machine learning classifiers used in our work for training and evaluating models. This facilitates a straightforward comparison of how varying hyperparameter selections influence the performance and reliability of the classifiers.

## IV. EXPERIMENTAL RESULTS

### A. EVALUATION METRICS

To assess the efficiency of the suggested method, different evaluation metrics are utilized. These measures include accuracy, precision, recall, and F1 score, which collectively provide a comprehensive evaluation of the method's effectiveness. The determination of these evaluation measures relies on the information provided by the confusion matrix, which contains the results of predictions, including true negatives (TN), false negatives (FN), true positives (TP), and false positives (FP) [48]. The mathematical representations of

**TABLE 5.** Dataset I Results of the four models' features without features concatenation or selection.

| Deep Features | ML Classifier | Accuracy Without Filtering | Performance Metrics | | | |
|---|---|---|---|---|---|---|
| | | | Accuracy | Precision | Recall | F1 Score |
| VGG-16 | SVM | 0.9047 | 0.9233 | 0.9098 | 0.9694 | 0.9387 |
| | RF | 0.8835 | 0.8995 | 0.8775 | 0.9694 | 0.9212 |
| | DT | 0.7751 | 0.7963 | 0.8276 | 0.8384 | 0.833 |
| | XGB | 0.8889 | 0.8942 | 0.8889 | 0.9432 | 0.9153 |
| Inception V3 | SVM | 0.8968 | 0.9153 | 0.9053 | 0.9607 | 0.9322 |
| | RF | 0.8492 | 0.8466 | 0.8379 | 0.9258 | 0.8797 |
| | DT | 0.7248 | 0.754 | 0.8091 | 0.7773 | 0.7929 |
| | XGB | 0.8915 | 0.9048 | 0.9038 | 0.9432 | 0.9231 |
| Resnet-101 | SVM | 0.9153 | **0.9259** | 0.9205 | 0.9607 | 0.9402 |
| | RF | 0.8730 | 0.8942 | 0.8795 | 0.9563 | 0.9163 |
| | DT | 0.7883 | 0.7884 | 0.8143 | 0.8428 | 0.8283 |
| | XGB | 0.9047 | **0.9259** | 0.9069 | 0.9782 | 0.9412 |
| DenseNet-201 | SVM | 0.8994 | 0.918 | 0.9091 | 0.9607 | 0.9342 |
| | RF | 0.8650 | 0.873 | 0.8549 | 0.952 | 0.9008 |
| | DT | 0.7407 | 0.7513 | 0.7897 | 0.8035 | 0.7965 |
| | XGB | 0.8835 | 0.8995 | 0.8866 | 0.9563 | 0.9202 |

**TABLE 6.** Dataset II Results of the four models' features without features concatenation or selection.

| Deep Features | ML Classifier | Accuracy Without Filtering | Performance Metrics | | | |
|---|---|---|---|---|---|---|
| | | | Accuracy | Precision | Recall | F1 Score |
| VGG-16 | SVM | 0.9462 | 0.9573 | 0.951 | 0.9645 | 0.9577 |
| | RF | 0.9491 | 0.9511 | 0.9422 | 0.9614 | 0.9517 |
| | DT | 0.8182 | 0.82 | 0.8223 | 0.8172 | 0.8198 |
| | XGB | 0.9302 | **0.9687** | 0.9669 | 0.9707 | 0.9688 |
| Inception V3 | SVM | 0.9497 | 0.9524 | 0.9537 | 0.9512 | 0.9525 |
| | RF | 0.8897 | 0.898 | 0.888 | 0.9113 | 0.8995 |
| | DT | 0.7908 | 0.7969 | 0.8032 | 0.7875 | 0.7953 |
| | XGB | 0.9391 | 0.9496 | 0.9475 | 0.9521 | 0.9498 |
| Resnet-101 | SVM | 0.9444 | 0.954 | 0.9475 | 0.9614 | 0.9544 |
| | RF | 0.9346 | 0.9438 | 0.9288 | 0.9614 | 0.9448 |
| | DT | 0.8368 | 0.8384 | 0.8413 | 0.835 | 0.8381 |
| | XGB | 0.9335 | 0.9409 | 0.936 | 0.9468 | 0.9413 |
| DenseNet-201 | SVM | 0.9315 | 0.9489 | 0.9486 | 0.9494 | 0.949 |
| | RF | 0.9588 | 0.9613 | 0.9557 | 0.9676 | 0.9616 |
| | DT | 0.8448 | 0.8549 | 0.8452 | 0.8696 | 0.8572 |
| | XGB | 0.9222 | 0.9351 | 0.9337 | 0.937 | 0.9353 |

the utilized metrics are as follows:

$$\text{Accuracy (ACC)} = \frac{TP + TN}{TP + TN + FP + FN} \tag{2}$$

$$\text{Precision (P)} = \frac{TP}{TP + FP} \tag{3}$$

$$\text{Recall (R)} = \frac{TP}{TP + FN} \tag{4}$$

$$\text{F1 score (F1)} = 2 \times \frac{P \times R}{P + R} \tag{5}$$

### B. EXPERIMENTAL SETUP

In our experimental setup, we employ four pre-trained deep CNN models, namely VGG-16, Inception V3, ResNext-101, and DenseNet-201, as feature extractors, which were pre-trained on the ImageNet dataset. Additionally, four different machine learning classifiers are utilized: SVM, RF, DT, and XGB. To prepare the input images, we apply pre-processing techniques and then extracting deep features. These features are then concatenated, and a genetic selection process is performed. All the experiments were carried out using a personal computer that was outfitted with an NVIDIA GeForce GTX 1070 graphics processing unit (GPU).

### C. RESULTS

The practical outcomes were derived from two distinct datasets (Dataset I and Dataset II) with the aim of detecting brain tumors. Once the preprocessing of the two MRI image datasets is completed, the preprocessed images serve as inputs to the pre-trained CNN models for the extraction of deep features. Multiple experiments are then conducted. In the first experiment, we utilized the extracted deep features from various pre-trained CNN networks, along with multiple Machine learning classifiers, without applying any feature

**TABLE 7.** Dataset I Results of the four models' features after features concatenation and selection.

| Deep Features | ML Classifier | Accuracy Without Filtering | Performance Metrics | | | |
|---|---|---|---|---|---|---|
| | | | Accuracy | Precision | Recall | F1 Score |
| VGG-16 | SVM | 0.9603 | 0.9841 | 1 | 0.9738 | 0.9867 |
| | RF | 0.9656 | 0.9709 | 0.9542 | 1 | 0.9765 |
| | DT | 0.9814 | 0.9841 | 0.9869 | 0.9869 | 0.9869 |
| | XGB | 0.9417 | 0.9841 | 0.9745 | 1 | 0.9871 |
| Inception V3 | SVM | 0.9735 | 0.9841 | 1 | 0.9738 | 0.9867 |
| | RF | 0.9470 | 0.955 | 0.9454 | 0.9825 | 0.9636 |
| | DT | 0.9259 | 0.9365 | 0.968 | 0.9258 | 0.9464 |
| | XGB | 0.9682 | 0.9788 | 1 | 0.9651 | 0.9822 |
| Resnet-101 | SVM | 0.9788 | 0.9894 | 1 | 0.9825 | 0.9912 |
| | RF | 0.9444 | 0.9577 | 0.9456 | 0.9869 | 0.9658 |
| | DT | 0.9603 | 0.9762 | 0.9741 | 0.9869 | 0.9805 |
| | XGB | 0.9417 | 0.9841 | 0.9745 | 1 | 0.9871 |
| DenseNet-201 | SVM | 0.9656 | 0.9709 | 1 | 0.952 | 0.9754 |
| | RF | 0.9523 | 0.9683 | 0.9617 | 0.9869 | 0.9741 |
| | DT | 0.9550 | 0.9683 | 0.9697 | 0.9782 | 0.9739 |
| | XGB | 0.9444 | 0.9815 | 0.9703 | 1 | 0.9849 |
| VGG-16+Inception V3 | SVM | 0.9761 | 0.9894 | 1 | 0.9825 | 0.9912 |
| | RF | 0.9365 | 0.9444 | 0.9262 | 0.9869 | 0.9556 |
| | DT | 0.9788 | 0.9815 | 0.9912 | 0.9782 | 0.9846 |
| | XGB | 0.9497 | 0.9841 | 0.9745 | 1 | 0.9871 |
| VGG-16+Inception V3+ResNet-101 | SVM | 0.9894 | **0.9974** | 1 | 0.9956 | 0.9978 |
| | RF | 0.9153 | 0.9206 | 0.8933 | 0.9869 | 0.9378 |
| | DT | 0.9417 | **0.9974** | 1 | 0.9956 | 0.9978 |
| | XGB | 0.9550 | 0.9868 | 0.9786 | 1 | 0.9892 |
| VGG16+Inception V3+ResNet-101+DenseNet-201 | SVM | 0.9894 | 0.9947 | 1 | 0.9913 | 0.9956 |
| | RF | 0.9206 | 0.9471 | 0.9231 | 0.9956 | 0.958 |
| | DT | 0.9708 | **0.9974** | 1 | 0.9956 | 0.9978 |
| | XGB | 0.9417 | 0.9868 | 0.9786 | 1 | 0.9892 |

concatenation or selection. The aim of this initial experiment is to provide an initial assessment of the performance of the extracted deep features using the pre-trained models. The outcomes of the initial experiment conducted on Dataset I and Dataset II are presented in Table 5 and Table 6. As indicated in Table 5 with the use of Dataset I, it can be observed that both the SVM and XGB classifiers demonstrated high performance, achieving an accuracy of 0.9259. This accuracy was attained by utilizing the deep features extracted from the ResNet-101 model. Similarly, based on our observation from Table 6 with the use of Dataset II, it is evident that the XGB classifier achieved high performance, attaining an accuracy of 0.9687. This accuracy was obtained by utilizing the extracted deep features using the VGG-16 model.

Based on the initial findings of the first experiment, we suggested that, by concatenating the deep features extracted from multiple CNN models, it can integrate diverse information captured by each model. Furthermore, employing a genetic selection algorithm to identify the most informative features subset from the concatenated deep features can lead to a substantial enhancement in performance.

In the second experiment, we utilized genetic feature selection algorithms for the extracted deep features using each of the four distinct CNN models individually. Moreover, we employed a concatenation process to merge the deep features obtained from these diverse CNN models, employing multiple levels of concatenation. Initially, we concatenated the extracted deep features from the first two models, namely VGG-16 and Inception V3. Subsequently, we proceeded to concatenate the features from the first three models, encompassing VGG-16, Inception V3, and ResNet-101. Finally, we performed a comprehensive concatenation that incorporated all the deep features extracted from the four models: VGG-16, Inception V3, ResNet-101, and DenseNet-201. Following the concatenation process, the genetic feature selection algorithm is applied to each level of concatenated features, meticulously evaluating and selecting the most relevant features. These selected features are then inputted into the different machine learning classifiers. The outcomes of the second experiment conducted on Dataset I and Dataset II are presented in Table 7 and Table 8.

Based on the findings presented in Table 7 using Dataset I, notable improvements are observed in the performance of each model after applying genetic selection to the extracted features from each CNN model. Also, it is evident that the SVM and DT classifiers exhibit the highest performance, Reaching an astounding accuracy of 0.9974. This exceptional accuracy was attained by leveraging the selected concatenated deep features extracted from the VGG-16, Inception V3, and ResNet-101 models. Similarly, the DT classifier achieved the same accuracy by utilizing the

**TABLE 8.** Dataset II Results of the four models' features after features concatenation and selection.

| Deep Features | ML Classifier | Accuracy Without Filtering | Performance Metrics | | | |
|---|---|---|---|---|---|---|
| | | | Accuracy | Precision | Recall | F1 Score |
| VGG-16 | SVM | 0.9744 | 0.9836 | 1 | 0.9672 | 0.9833 |
| | RF | 0.9586 | 0.9756 | 0.9669 | 0.9849 | 0.9758 |
| | DT | 0.9780 | 0.9847 | 0.9932 | 0.976 | 0.9846 |
| | XGB | 0.9684 | 0.9858 | 0.9991 | 0.9725 | 0.9856 |
| Inception V3 | SVM | 0.9664 | 0.9833 | 1 | 0.9667 | 0.9831 |
| | RF | 0.9551 | 0.9744 | 0.9714 | 0.9778 | 0.9746 |
| | DT | 0.9662 | 0.9849 | 0.974 | 0.9965 | 0.9851 |
| | XGB | 0.9731 | 0.9831 | 1 | 0.9663 | 0.9829 |
| Resnet-101 | SVM | 0.9664 | 0.9833 | 1 | 0.9667 | 0.9831 |
| | RF | 0.9735 | 0.9871 | 0.9828 | 0.9916 | 0.9872 |
| | DT | 0.9617 | 0.9887 | 0.9928 | 0.9845 | 0.9886 |
| | XGB | 0.9642 | 0.9751 | 1 | 0.9503 | 0.9745 |
| DenseNet-201 | SVM | 0.9664 | 0.9833 | 1 | 0.9667 | 0.9831 |
| | RF | 0.9768 | 0.9884 | 0.9885 | 0.9885 | 0.9885 |
| | DT | 0.9724 | 0.9867 | 0.9741 | 1 | 0.9869 |
| | XGB | 0.9620 | 0.9853 | 1 | 0.9707 | 0.9851 |
| VGG-16+Inception V3 | SVM | 0.9671 | 0.9836 | 1 | 0.9672 | 0.9833 |
| | RF | 0.9788 | 0.9858 | 0.9862 | 0.9854 | 0.9858 |
| | DT | 0.9815 | 0.99 | 0.9929 | 0.9871 | 0.9899 |
| | XGB | 0.9802 | 0.992 | 1 | 0.984 | 0.9919 |
| VGG-16+Inception V3+Resnet101 | SVM | 0.9982 | 0.9982 | 1 | 0.9965 | 0.9982 |
| | RF | 0.9864 | 0.9949 | 0.9925 | 0.9973 | 0.9949 |
| | DT | 0.9880 | **0.9987** | 0.9996 | 0.9978 | 0.9987 |
| | XGB | 0.9784 | 0.9931 | 1 | 0.9862 | 0.9931 |
| VGG-16+Inception V3+Resnet-101+DenseNet-201 | SVM | 0.9982 | 0.9982 | 1 | 0.9965 | 0.9982 |
| | RF | 0.9704 | 0.9924 | 0.9912 | 0.9938 | 0.9925 |
| | DT | 0.9833 | 0.9902 | 0.9924 | 0.988 | 0.9902 |
| | XGB | 0.9797 | 0.9971 | 1 | 0.9942 | 0.9971 |

**TABLE 9.** Dataset I time analysis.

| Process | | Time (Min) |
|---|---|---|
| Preprocessing | | 0.141 |
| Feature Extraction | VGG-16 | 1.087 |
| | Inception V3 | 1.124 |
| | Resnet-101 | 1.537 |
| | DenseNet-201 | 1.308 |
| Feature Concatenation | VGG-16+Inception V3 | 0.039 |
| | VGG-16+InceptionV3+ResNet-101 | 0.068 |
| | VGG16+InceptionV3+ResNet-101+DenseNet-201 | 0.104 |
| Feature Selection | VGG-16 | 0.205 |
| | Inception V3 | 0.293 |
| | Resnet-101 | 0.295 |
| | DenseNet-201 | 0.288 |
| | VGG-16+InceptionV3 | 0.333 |
| | VGG-16+InceptionV3+ResNet-101 | 0.486 |
| | VGG16+InceptionV3+ResNet-101+DenseNet-201 | 0.635 |
| Classification | VGG-16 | 0.01 |
| | Inception V3 | 0.044 |
| | Resnet-101 | 0.038 |
| | DenseNet-201 | 0.032 |
| | VGG-16+InceptionV3 | 0.037 |
| | VGG-16+InceptionV3+ResNet-101 | 0.069 |
| | VGG16+InceptionV3+ResNet-101+DenseNet-201 | 0.124 |

**TABLE 10.** Dataset II time analysis.

| Process | | Time (Min) |
|---|---|---|
| Preprocessing | | 1.1852 |
| Feature Extraction | VGG-16 | 17.425 |
| | Inception V3 | 18.184 |
| | Resnet-101 | 15.921 |
| | DenseNet-201 | 20.203 |
| Feature Concatenation | VGG-16+Inception V3 | 0.457 |
| | VGG-16+InceptionV3+ResNet-101 | 0.822 |
| | VGG16+InceptionV3+ResNet-101+DenseNet-201 | 1.227 |
| Feature Selection | VGG-16 | 0.222 |
| | Inception V3 | 0.442 |
| | Resnet-101 | 0.437 |
| | DenseNet-201 | 0.407 |
| | VGG-16+InceptionV3 | 0.520 |
| | VGG-16+InceptionV3+ResNet-101 | 0.894 |
| | VGG16+InceptionV3+ResNet-101+DenseNet-201 | 1.147 |
| Classification | VGG-16 | 0.064 |
| | Inception V3 | 0.354 |
| | Resnet-101 | 0.318 |
| | DenseNet-201 | 0.267 |
| | VGG-16+InceptionV3 | 0.427 |
| | VGG-16+InceptionV3+ResNet-101 | 1.111 |
| | VGG16+InceptionV3+ResNet-101+DenseNet-201 | 1.224 |

selected concatenated deep features extracted from all four models.

Additionally, as presented in Table 8 when utilizing Dataset II, it is clear that there is a substantial enhancement in the performance of each model after applying genetic selection to the extracted features from each individual CNN model. Notably, it is evident that the DT classifier achieves the highest performance, attaining an impressive accuracy

**TABLE 11. Comparison with similar related works.**

| Ref | Dataset | Accuracy (%) | Limitations | How Limitations Are Overcome by Our Method |
|---|---|---|---|---|
| Saxena et al. [22] | Dataset I | 95 | Only one dataset was utilized and obtained Lower accuracy compared to our method | Our method utilizes two distinct datasets and achieves remarkable accuracy enhancement |
| Kang et al. [26] | Dataset I | 98.04 | Applied preliminary classification to select optimal features relies on average accuracy, which might not be precise due to variations in accuracy across different algorithms | Our method uses a selection technique that offers global optimization across wide solution spaces to choose the most relevant and informative characteristics from the initial concatenated feature set |
| Kang et al. [26] | Dataset II | 98.83 | Applied preliminary classification to select optimal features relies on average accuracy, which might not be precise due to variations in accuracy across different algorithms | Our method uses a selection technique that offers global optimization across wide solution spaces to choose the most relevant and informative characteristics from the initial concatenated feature set |
| Ozbay and Ozbay [27] | Dataset II | 99.6 | Employed a features selection technique that only focuses locally on relevance and coherence to identify the most informative features | Our method uses a selection technique that offers global optimization across wide solution spaces to choose the most relevant and informative characteristics from the initial concatenated feature set |
| Mahmoud et al. [28] | Dataset II | 98.95 | Only one dataset was utilized and obtained Lower accuracy compared to our method | Our method utilizes two distinct datasets and achieves remarkable accuracy enhancement |
| Proposed | Dataset I | 99.74 | Further refining is required to classify distinct forms of brain tumors | Our method outperformed others, demonstrating superior accuracy by the utilization of feature concatenation and genetic selection techniques |
| Proposed | Dataset II | 99.87 | Further refining is required to classify distinct forms of brain tumors | Our method outperformed others, demonstrating superior accuracy by the utilization of feature concatenation and genetic selection techniques |

of 0.9987. This exceptional accuracy is accomplished by utilizing the selected concatenated deep features extracted from the VGG-16, Inception V3, and ResNet-101 models. Furthermore, the impressive performance highlights the robustness of the features extracted from various pre-trained CNN models under different conditions, confirming the reliability and quality of the features in our proposed method.

In addition, in both the initial and subsequent experiments, the accuracy of both datasets was evaluated without implementing any filtering techniques on the MRI images. This step was crucial to assess the impact of the filtering process on model performance. Consequently, Tables 5, 6, 7, and 8 present the accuracy results obtained without filtering. The observed results indicate an improvement in the accuracy after applying the filtering processes to the MRI images. This underscores the significant role of filtering in enhancing model performance, demonstrating its effectiveness in improving the overall accuracy and reliability of the outcomes.

Based on our findings, it is observed that optimal performance is achieved through the concatenated features of the first three models (VGG-16, Inception V3, and ResNet-101) rather than incorporating all four models (VGG-16, Inception V3, ResNet-101, and DenseNet-201). This suggests that superior performance is attained by leveraging a smaller subset of features that means speeding up processing times and reducing resources and storage consumption.

For a more comprehensive analysis, Table 9 and Table 10 provide the time analysis for Dataset I and Dataset II, respectively, across various stages: preprocessing, feature extraction, feature concatenation, feature selection, and classification. It is observed that the processing times for Dataset I are shorter than those for Dataset II, particularly in the feature extraction and selection stages. This is primarily attributed to the significantly larger size of Dataset II, especially After the augmentation process. The time required for feature extraction and selection is considerably higher in Dataset II due to the increased computational complexity associated with handling a larger volume of data. Additionally, the variation in processing times can also be influenced by the specific models utilized. Models with more complex architectures tend to require more time for both feature extraction and selection. This detailed time analysis underscores the importance of considering dataset size and model complexity when evaluating the efficiency and scalability of different workflows. Also, employing parallel processing and

distributed computing methods could significantly decrease the time required for extensive datasets.

In comparison to previous related works, our research represents significant performance in the domain of brain tumor detection. Table 11 presents a comparison of our results with previous related works by Saxena et al. [22], Kang et al. [26], Ozbay and Ozbay [27], Mahmoud et al. and [28] that utilized the same datasets. The observations from Table 11 reveal that our proposed method exhibited superior performance with higher accuracy compared to the other related works achieving accuracy that reached 99.74% using Dataset I and 99.87% using Dataset II. Furthermore, our proposed method also surpasses the other methods across the other metrics. Additionally, our suggested method attempted to address some of the current drawbacks, including comparatively limited size datasets, heterogeneity and feature scattering, and redundant and irrelevant information. Our method advantages can be spotlighted as follows:

- Utilizing hybrid method for brain tumor detection to overcome the relatively small datasets by using different pre-trained CNN models to extract deep features from brain MRI images and employing machine learning classifiers to effectively detect brain tumor in MRI images.
- Enhancing Feature representation and overcoming heterogeneity and feature scattering by depending on a concatenated deep feature vector which combines the deep features extracted from the distinct pre-trained CNN models to combine diverse visual information and obtain more comprehensive feature representation.
- Reducing feature redundancy, irrelevancy, and dimensionality by applying the genetic algorithm as a feature selection technique to identify and utilize the most powerful and important features, also lowering the expense of computing.
- Two distinct MRI datasets have been used to evaluate our proposed method for the brain tumor detection and it has demonstrated high accuracy using both datasets.

These findings highlight the superior efficacy of our proposed method when compared to the other methods, emphasizing its potential for enhancing outcomes in this field.

## V. CONCLUSION

Brain tumor can develop at any age and lead to the deterioration of brain cell structures. Early detection of brain tumors is extremely important, not only for halting the advancement of the disease but also for significantly enhancing the quality of life for those affected. In this research, our primary objective is to develop an efficient methodology for early detection of brain tumors based on MRI. By incorporating transfer learning and leveraging multiple pre-trained deep CNN models, we successfully extracted deep features from brain MRI images. Two experiments were conducted to assess the effectiveness of the extracted features. In the first experiment, deep features from various pre-trained CNN networks were used with multiple machine learning classifiers without applying feature concatenation or selection, resulting in an accuracy of 92.59% and 96.87% on the first and second datasets, respectively. The second experiment involved feature concatenation to integrate diverse information from different models and feature selection to identify the most relevant and significant features from the concatenated deep features extracted by the four CNN models. The combination of deep features particularly those from the first three models resulted in a significant enhancement in performance resulted in a significant enhancement in performance, reaching an impressive accuracy level of 99.74% and 99.87% on the first and second datasets, respectively. These outcomes underscore the effectiveness of our method in precisely detecting brain tumors, which has the potential to greatly assist doctors and specialists in early diagnosis and subsequent treatment planning.

Future research directions could involve expanding the evaluation to encompass larger and more diverse datasets, thereby ensuring a comprehensive understanding of the method's applicability across different scenarios. Additionally, exploring a variety of deep learning architectures could provide insights into the most effective models for this application. Conducting clinical trials will be crucial to validate the efficiency and reliability of the proposed method. Furthermore, it is essential to refine the technique to enhance its ability to accurately classify distinct forms of brain tumors, which would significantly improve diagnostic precision and treatment planning. Also, utilizing parallel processing and distributed computing techniques could substantially reduce the time needed for large datasets and models with more intricate architectures.

## ACKNOWLEDGMENT

The authors would like to express their thanks to Princess Nourah Bint Abdulrahman University Researchers Supporting. They would also like to extend their sincere gratitude to Prof. Ashraf A. Zayton from the Radiodiagnosis Department, Faculty of Medicine, Menofia University, Egypt, for his invaluable assistance and expert consultations on medical aspects and magnetic resonance imaging. His insights and guidance have significantly contributed to the success of this research.

## REFERENCES

[1] A. H. Khan, S. Abbas, M. A. Khan, U. Farooq, W. A. Khan, S. Y. Siddiqui, and A. Ahmad, "Intelligent model for brain tumor identification using deep learning," *Appl. Comput. Intell. Soft Comput.*, vol. 2022, pp. 1–10, Jan. 2022.

[2] A. R. Mathew, P. B. Anto, and N. K. Thara, "Brain tumor segmentation and classification using DWT, gabour wavelet and GLCM," in *Proc. Int. Conf. Intell. Comput., Instrum. Control Technol. (ICICICT)*, Jul. 2017, pp. 1744–1750.

[3] D. N. Louis, A. Perry, G. Reifenberger, A. von Deimling, D. Figarella-Branger, W. K. Cavenee, H. Ohgaki, O. D. Wiestler, P. Kleihues, and D. W. Ellison, "The 2016 World Health Organization classification of tumors of the central nervous system: A summary," *Acta Neuropathologica*, vol. 131, no. 6, pp. 803–820, Jun. 2016.

[4] S. J. Choi, J. S. Kim, J. H. Kim, S. J. Oh, J. G. Lee, C. J. Kim, Y. S. Ra, J. S. Yeo, J. S. Ryu, and D. H. Moon, "[$^{18}$F]3'-deoxy-3'-fluorothymidine PET for the diagnosis and grading of brain tumors," *Eur. J. Nucl. Med. Mol. Imag.*, vol. 32, no. 6, pp. 653–659, Jun. 2005.
[5] S. Pereira, A. Pinto, V. Alves, and C. A. Silva, "Brain tumor segmentation using convolutional neural networks in MRI images," *IEEE Trans. Med. Imag.*, vol. 35, no. 5, pp. 1240–1251, May 2016.
[6] K. Popuri, D. Cobzas, A. Murtha, and M. Jägersand, "3D variational brain tumor segmentation using Dirichlet priors on a clustered feature set," *Int. J. Comput. Assist. Radiol. Surg.*, vol. 7, no. 4, pp. 493–506, Jul. 2012.
[7] N. Varuna Shree and T. N. R. Kumar, "Identification and classification of brain tumor MRI images with feature extraction using DWT and probabilistic neural network," *Brain Informat.*, vol. 5, no. 1, pp. 23–30, Mar. 2018.
[8] Z. Ullah, M. U. Farooq, S.-H. Lee, and D. An, "A hybrid image enhancement based brain MRI images classification technique," *Med. Hypotheses*, vol. 143, Oct. 2020, Art. no. 109922.
[9] P. G. Rajan and C. Sundar, "Brain tumor detection and segmentation by intensity adjustment," *J. Med. Syst.*, vol. 43, no. 8, pp. 1–13, Aug. 2019.
[10] M. Arunachalam and S. R. Savarimuthu, "An efficient and automatic glioblastoma brain tumor detection using shift-invariant shearlet transform and neural networks," *Int. J. Imag. Syst. Technol.*, vol. 27, no. 3, pp. 216–226, Sep. 2017.
[11] N. Gupta, P. Bhatele, and P. Khanna, "Glioma detection on brain MRIs using texture and morphological features with ensemble learning," *Biomed. Signal Process. Control*, vol. 47, pp. 115–125, Jan. 2019.
[12] A. Minz and C. Mahobiya, "MR image classification using AdaBoost for brain tumor type," in *Proc. IEEE 7th Int. Advance Comput. Conf. (IACC)*, Jan. 2017, pp. 701–705.
[13] N. Zulpe and V. Pawar, "GLCM textural features for brain tumor classification," *Int. J. Comput. Sci. Issues*, vol. 9, no. 3, p. 354, 2012.
[14] P. R. E. Arasi and M. Suganthi, "A clinical support system for brain tumor classification using soft computing techniques," *J. Med. Syst.*, vol. 43, no. 5, pp. 1–11, May 2019.
[15] M. Soltaninejad, G. Yang, T. Lambrou, N. Allinson, T. L. Jones, T. R. Barrick, F. A. Howe, and X. Ye, "Automated brain tumour detection and segmentation using superpixel-based extremely randomized trees in FLAIR MRI," *Int. J. Comput. Assist. Radiol. Surg.*, vol. 12, no. 2, pp. 183–203, Feb. 2017.
[16] N. Nabizadeh and M. Kubat, "Automatic tumor segmentation in single-spectral MRI using a texture-based and contour-based algorithm," *Expert Syst. Appl.*, vol. 77, pp. 1–10, Jul. 2017.
[17] M. Wageh, K. Amin, A. Zytoon, and M. Ibrahim, "Brain tumor detection based on a combination of GLCM and LBP features with PCA and IG," *Int. J. Comput. Inf.*, vol. 10, no. 2, pp. 43–53, 2023.
[18] N. Abiwinanda, M. Hanif, S. T. Hesaputra, A. Handayani, and T. R. Mengko, "Brain tumor classification using convolutional neural network," in *Proc. World Congr. Med. Phys. Biomed. Eng.*, vol. 1, Prague, Czech Republic, Jun. 2019, pp. 183–189.
[19] S. Deepak and P. M. Ameer, "Brain tumor classification using deep CNN features via transfer learning," *Comput. Biol. Med.*, vol. 111, Aug. 2019, Art. no. 103345.
[20] A. Çinar and M. Yildirim, "Detection of tumors on brain MRI images using the hybrid convolutional neural network architecture," *Med. Hypotheses*, vol. 139, Jun. 2020, Art. no. 109684.
[21] S. Khawaldeh, U. Pervaiz, A. Rafiq, and R. Alkhawaldeh, "Noninvasive grading of glioma tumor using magnetic resonance imaging with convolutional neural networks," *Appl. Sci.*, vol. 8, no. 1, p. 27, Dec. 2017.
[22] P. Saxena, A. Maheshwari, and S. Maheshwari, "Predictive modeling of brain tumor: A deep learning approach," in *Innovations in Computational Intelligence and Computer Vision*. Cham, Switzerland: Springer, 2020, pp. 275–285.
[23] Z. N. K. Swati, Q. Zhao, M. Kabir, F. Ali, Z. Ali, S. Ahmed, and J. Lu, "Brain tumor classification for MR images using transfer learning and fine-tuning," *Computerized Med. Imag. Graph.*, vol. 75, pp. 34–46, Jul. 2019.
[24] F. J. Díaz-Pernas, M. Martínez-Zarzuela, M. Antón-Rodríguez, and D. González-Ortega, "A deep learning approach for brain tumor classification and segmentation using a multiscale convolutional neural network," *Healthcare*, vol. 9, no. 2, p. 153, Feb. 2021.
[25] N. Noreen, S. Palaniappan, A. Qayyum, I. Ahmad, and M. O. Alassafi, "Brain tumor classification based on fine-tuned models and the ensemble method," *Comput., Mater. Continua*, vol. 67, no. 3, pp. 3967–3982, 2021.
[26] J. Kang, Z. Ullah, and J. Gwak, "MRI-based brain tumor classification using ensemble of deep features and machine learning classifiers," *Sensors*, vol. 21, no. 6, p. 2222, Mar. 2021.
[27] F. A. Özbay and E. Özbay, "Brain tumor detection with mRMR-based multimodal fusion of deep learning from MR images using grad-CAM," *Iran J. Comput. Sci.*, vol. 6, no. 3, pp. 245–259, Sep. 2023.
[28] A. Mahmoud, N. A. Awad, N. Alsubaie, S. I. Ansarullah, M. S. Alqahtani, M. Abbas, M. Usman, B. O. Soufiene, and A. Saber, "Advanced deep learning approaches for accurate brain tumor classification in medical imaging," *Symmetry*, vol. 15, no. 3, p. 571, Feb. 2023.
[29] S. Anantharajan, S. Gunasekaran, and T. Subramanian, "MRI brain tumor detection using deep learning and machine learning approaches," *Measurement, Sensors*, vol. 31, Feb. 2024, Art. no. 101026.
[30] T. Rahman and M. S. Islam, "MRI brain tumor detection and classification using parallel deep convolutional neural networks," *Measurement, Sensors*, vol. 26, Apr. 2023, Art. no. 100694.
[31] M. Z. Khaliki and M. S. Başarslan, "Brain tumor detection from images and comparison with transfer learning methods and 3-layer CNN," *Sci. Rep.*, vol. 14, no. 1, p. 2664, Feb. 2024.
[32] S. Ghanavati, J. Li, T. Liu, P. S. Babyn, W. Doda, and G. Lampropoulos, "Automatic brain tumor detection in magnetic resonance images," in *Proc. 9th IEEE Int. Symp. Biomed. Imag. (ISBI)*, May 2012, pp. 574–577.
[33] N. Chakrabarty, "Brain MRI images for brain tumor detection," *J. Exp. Med.*, vol. 216, pp. 539–555, Jan. 2019. [Online]. Available: https://www.kaggle.com/datasets/navoneel/brain-mri-images-for-brain-tumor-detection
[34] A. Hamada. (2020). *Br35H :: Brain Tumor Detection 2020*. [Online]. Available: https://www.kaggle.com/datasets/ahmedhamada0/brain-tumor-detection
[35] D. M. Kumar, D. Satyanarayana, and M. N. G. Prasad, "MRI brain tumor detection using optimal possibilistic fuzzy C-means clustering algorithm and adaptive k-nearest neighbor classifier," *J. Ambient Intell. Humanized Comput.*, vol. 12, no. 2, pp. 2867–2880, Feb. 2021.
[36] M. Goyal, R. Goyal, and B. Lall, "Learning activation functions: A new paradigm for understanding neural networks," 2019, *arXiv:1906.09529*.
[37] S. Albawi, T. A. Mohammed, and S. Al-Zawi, "Understanding of a convolutional neural network," in *Proc. Int. Conf. Eng. Technol. (ICET)*, Aug. 2017, pp. 1–6.
[38] S. Christodoulidis, M. Anthimopoulos, L. Ebner, A. Christe, and S. Mougiakakou, "Multisource transfer learning with convolutional neural networks for lung pattern analysis," *IEEE J. Biomed. Health Informat.*, vol. 21, no. 1, pp. 76–84, Jan. 2017.
[39] S. J. Pan and Q. Yang, "A survey on transfer learning," *IEEE Trans. Knowl. Data Eng.*, vol. 22, no. 10, pp. 1345–1359, Oct. 2010, doi: 10.1109/TKDE.2009.191.
[40] K. Simonyan and A. Zisserman, "Very deep convolutional networks for large-scale image recognition," 2014, *arXiv:1409.1556*.
[41] C. Szegedy, V. Vanhoucke, S. Ioffe, J. Shlens, and Z. Wojna, "Rethinking the inception architecture for computer vision," in *Proc. IEEE Conf. Comput. Vis. Pattern Recognit. (CVPR)*, Jun. 2016, pp. 2818–2826.
[42] K. He, X. Zhang, S. Ren, and J. Sun, "Deep residual learning for image recognition," in *Proc. IEEE Conf. Comput. Vis. Pattern Recognit. (CVPR)*, Jun. 2016, pp. 770–778.
[43] G. Huang, Z. Liu, L. Van Der Maaten, and K. Q. Weinberger, "Densely connected convolutional networks," in *Proc. IEEE Conf. Comput. Vis. Pattern Recognit. (CVPR)*, Jul. 2017, pp. 2261–2269.
[44] D. M. Alawad, A. Mishra, and M. T. Hoque, "AIBH: Accurate identification of brain hemorrhage using genetic algorithm based feature selection and stacking," *Mach. Learn. Knowl. Extraction*, vol. 2, no. 2, pp. 56–77, Apr. 2020.
[45] P. S. Chander, J. Soundarya, and R. Priyadharsini, "Brain tumour detection and classification using K-means clustering and SVM classifier," in *Proc. 6th Int. Conf. Robot Intell. Technol. Appl.*, 2018, pp. 49–63.
[46] G. Garg and R. Garg, "Brain tumor detection and classification based on hybrid ensemble classifier," 2021, *arXiv:2101.00216*.
[47] A. Hashmi and A. H. Osman, "Brain tumor classification using conditional segmentation with residual network and attention approach by extreme gradient boost," *Appl. Sci.*, vol. 12, no. 21, p. 10791, Oct. 2022.
[48] M. Sokolova and G. Lapalme, "A systematic analysis of performance measures for classification tasks," *Inf. Process. Manage.*, vol. 45, no. 4, pp. 427–437, Jul. 2009.

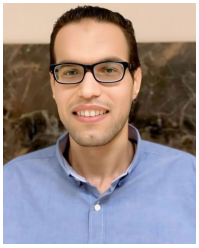

**MOHAMED WAGEH** received the B.Sc. degree (Hons.) in information technology from the Faculty of Computers and Information, Menofia University, Menofia, Egypt, in 2016. He is currently an Assistant Lecturer with the Faculty of Computers and Information, Menoufia University. His research interests include brain tumors, computer vision, machine learning, and deep learning.

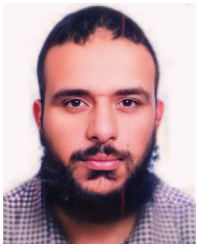

**KHALID AMIN** received the Ph.D. degree in electronics from the Faculty of Engineering, Ain Shams University, Egypt, in 2006. He is a Professor and the Head of the Department of Information Technology, Faculty of Computers and Information, Menofia University, Egypt. His working areas include medical image processing, digital signal processing, and speech recognition. He has published more than 35 papers in international journals and conferences.

**ABEER D. ALGARNI** received the B.Sc. degree (Hons.) in computer science from King Saud University, Riyadh, Saudi Arabia, in 2007, and the M.Sc. and Ph.D. degrees from the School of Engineering and Computer Sciences, Durham University, U.K., in 2010 and 2015, respectively. She has been an Assistant Professor with the College of Computer and Information Sciences, Princess Nourah Bint Abdulrahman University, since 2008. Her current research interests include networking and communication systems, digital image processing, digital communications, and cyber security.

**AHMED M. HAMAD** was born in Menoufia, Egypt, in October 1978. He received the B.Sc. and M.Sc. degrees in information technology from Cairo University, Egypt, in 2000 and 2005, respectively, and the Ph.D. degree in information science from the Graduate School of Advanced Integration Science, Chiba University, Japan, in March 2012. In 2012, he joined the Department of Information Technology, Faculty of Computers and Information, Menoufia University, as an Assistant Professor. His research interests include object detection in videos, human fall detection, human action recognition and analysis in videos, crowd analysis, and transferring videos on concurrent multipaths.

**MINA IBRAHIM** received the M.Sc. degree in computers and information (information technology) from Menoufia University, Menoufia, Egypt, in 2006, and the Ph.D. degree in electronics and electrical engineering from Southampton University, England, U.K., in 2012. Currently, he is an Associate Professor with the Faculty of Artificial Intelligence, Menoufia University.